

Simple Design of Edge-Emitting Diode Laser to Overcome Thermal Lens Effect

N. N. Elkin, A. P. Napartovich, *Member IEEE*, and D. V. Vysotsky
 SRC RF Troitsk Institute for Innovation and Thermonuclear Research
 Pushkovykh prop. 12
 Troitsk, Moscow province, 142190 Russia, elkin@triniti.ru

Abstract— Parameters of two-element, index-guided laser structure providing single-mode operation at high power are found numerically. 3-D numerical code has been implemented, which takes into account carrier diffusion in the quantum well, edge radiation losses and thermal lens effect. Within the simulation, higher-order optical modes on a ‘frozen background’ are computed. The onset of threshold for higher-order modes puts an upper limit on the range for stable, single-mode operation. Then, for the 5 μm-core and 2 mm-length device, stable, single-mode operation up to Watt-level output power is predicted with laser efficiency growing as a function of drive currents.

I. INTRODUCTION

There is an increasing need for single-spatial-mode, 0.98 μm-emitting semiconductor lasers with reliable cw output powers in excess of 1 W for applications such as pumps for rare-earth-doped fiber amplifiers (in fiber-optical communications) and free-space communications. Common positive-index-guided devices are limited by thermally induced kinks to stable, single-mode operation up to the 800 mW-1 W cw range. Such devices have relatively small lasing-spot (lateral) widths: 4-5 μm. In turn, that limits the reliability of fully facet-passivated devices (due to bulk degradation) to around 700 mW. However, conventional devices of ~10 μm-wide lasing spot suffer from the appearance of additional lasing modes that cause degradation in optical-beam quality. The mechanisms responsible for the onset of such multimoding are well known: gain spatial hole burning (GSHB) and self-focusing/defocusing associated with carrier- and thermally-induced index variations.

An idea to fight against this phenomenon is to design hetero-structure in order to invert fundamental mode profile – replace maximum at the center by a minimum. Then, thermal lens leads to flattening of mode’s profile, which increases stability against the GSHB [1]. To realize this idea, parameters of the hetero-structure should be carefully selected. We demonstrate numerically in this work an example of two-element, index-guided laser structure that its parameters properly selected can provide high stability of single-mode operation.

II. NUMERICAL MODEL

Overviews of different approaches for modeling diode lasers can be found in [2, 3]. The optical subroutine of a model employed here is described in detail in [4]. Wave field in a laser is described by the scalar Helmholtz equation. The beam propagation method has been chosen. The Helmholtz equation solver is realized in wide-angle approximation of Ref. [5] for counter propagating beams with amplitudes E_+ and E_- . Standard boundary conditions (reflection of the beam) are imposed at the end facets. The PML boundary conditions [6] for vertical and lateral boundaries have been implemented.

For describing the interaction between the wave field and the carriers in the quantum well (QW) we use an approach based on the 1D diffusion equation [2] for the carrier density N :

$$\frac{\partial^2 Y}{\partial y^2} - \frac{Y}{D\tau_{nr}} - \frac{B}{D} N_{tr} Y^2 - \frac{(|E_+|^2 + |E_-|^2)g}{g_{0N}D\tau_{nr}} = -\frac{j}{qDd_w N_{tr}}, \quad (1)$$

where $Y = N/N_{tr}$, $N_{tr} = \left(-\tau_{nr}^{-1} + \sqrt{\tau_{nr}^{-2} + 4Bj_{tr}/qd_w} \right) / (2B)$,

$|E_+|^2 + |E_-|^2 = I/I_s$, $I_s = (hcN_{tr})/(\lambda g_{0N}\tau_{nr})$, y is a lateral coordinate, N_{tr} is the carrier number density for conditions of QW transparency, D is the carrier diffusion coefficient, τ_{nr} is the non-radiative recombination time, B is the spontaneous emission coefficient, j is the drive-current density, q is the electron charge, d_w is the QW thickness, j_{tr} is the drive-current density at the transparency conditions, I_s is the saturation intensity, and hc/λ is the energy quantum. The gain coefficient g as a function of N was approximated by a logarithmic-type approximation [7] containing a gain parameter g_{0N} . Description of the thermal subroutine for computing temperature spatial distribution is given in [7]. Heating rate terms include the ohmic loss and the thermalization effect of electrons and holes in the QW. The refraction index n includes thermal variations and non-linear term within the QW [7]. The thermo-optic coefficient was taken equal to $3 \cdot 10^{-4} \text{ K}^{-1}$.

Fox-Li iteration method is implemented to find an oscillating mode self-consistently with the spatial temperature profile and carrier density distribution at a prescribed drive-current profile in the QW plane.

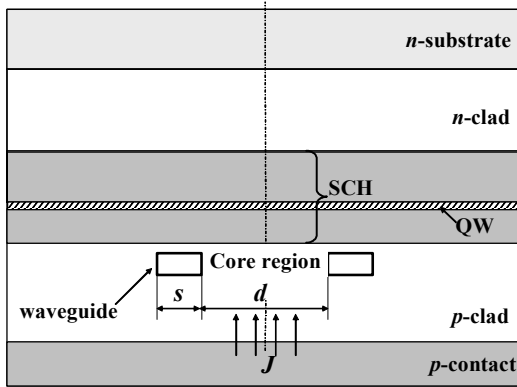


Fig. 1. Schematic drawing of two-element, index-guided active zone.

To calculate a critical drive level, at which additional modes appear, the numerical code incorporates a subroutine, which calculates a set of competing modes using gain and index variations produced by the oscillating mode. The modal gains of the competing modes grow with drive current due to the GSHB and thermal lens effects, and overcome the threshold at some current level. The corresponding linear eigen-value problem is solved by the Arnoldi method [8] which finds a set of optical modes.

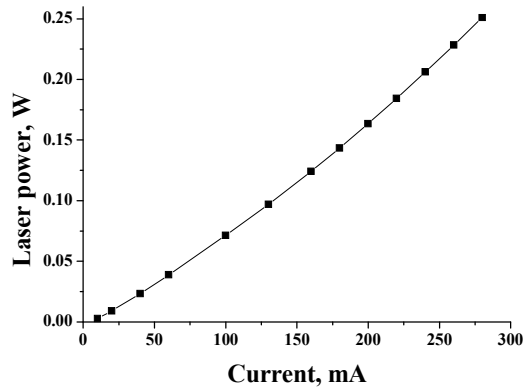


Fig. 2. Output power vs drive current, $t=0.1 \mu\text{m}$, $s=0.6 \mu\text{m}$, $L=0.2 \text{ mm}$.

III. RESULTS AND DISCUSSION

Schematic representation of the two-element, index-guided structure is shown in Fig. 1. The injected current was assumed for the numerical simulations to be distributed uniformly across the core of wide d . The transverse structure is of the separate-confinement-heterostructure (SCH)-type, with one quantum well, and is designed to have a low transverse optical-mode confinement factor, $\Gamma \sim 1\%$ for reduced GSHB and subsequent increased high-power, single-mode capability [9]. The mirror's reflectance and parameters entered into the carrier-diffusion equation (1) were set as follows: $r_1=0.95$, $r_2=0.01$ for the device length $L=2 \text{ mm}$, $r_1=0.995$, $r_2=0.631$ for $L=0.2 \text{ mm}$, $j_{\text{tr}}=50 \text{ A}\cdot\text{cm}^{-2}$, $g_{0N}=2200 \text{ cm}^{-1}$, $B=10^{10} \text{ cm}^3\text{s}^{-1}$, $R=2$, $\tau_{\text{nr}}=1 \text{ ns}$, $D=100 \text{ cm}^2\text{s}^{-1}$, $d_w=8.5 \text{ nm}$. The boundary conditions in thermal subroutine reflect three thermally isolated facets and fixed temperature on cooler side.

We expect that the device length weakly influences on its modal properties. Purposely to reduce computational costs, the

parameters search was performed for the device of $L=0.2 \text{ mm}$ with mirrors' reflection coefficients ensuring self-similarity [4].

Our purpose is to find s , t parameters providing gain/loss balance for the fundamental guided mode better than for the leaky mode. Such conditions, in terms of the effective index [2], were found analytically in [1]. Series of calculations for short devices demonstrated that $t=0.1 \mu\text{m}$ and s values between 0.6 and $1.0 \mu\text{m}$ lead to the fundamental guided mode dominance. A laser power vs drive current for a device of 0.2 mm length, $s=0.6 \mu\text{m}$, and $d=5 \mu\text{m}$ is shown in Fig. 2. In contrast to conventional devices, this power rises accelerated up to the drive current $J=280 \text{ mA}$ (current density is 28 kA/cm^2 , maximum temperature increment is 26.3 K , output power is 251 mW). The fundamental mode width is about $8 \mu\text{m}$. Higher-order modes calculations confirm that there is no trend for these modes to approach the threshold.

Further search of optimal device parameters gives the following results for the 2 mm -length device with $t=0.1 \mu\text{m}$, $s=1 \mu\text{m}$, $d=8 \mu\text{m}$. At the drive current 2.64 A the output single-mode power achieved 2.46 W , the maximum temperature rise was 21.3 K .

ACKNOWLEDGMENT

The authors thank V. N. Troshchieva for her assistance in computer simulation.

REFERENCES

- [1] D.V. Vysotsky, N.N. Elkin, A.P. Napartovich, "Active composite waveguides with a suppressed competition of optical modes," *Quantum Electronics*, vol. 38, pp. 707 – 709, 2008
- [2] G. R. Hadley, "Modeling of diode laser arrays," Chapter 4 in *Diode Laser Arrays*, D. Botez and D. R. Scifres, Eds., Cambridge, U.K., Cambridge Univ. Press, 1994, pp. 180–225.
- [3] R. Scarmozzino, A. Gopinath, R. Pregla, and S. Helfert, "Numerical techniques for modeling guided-wave photonic devices," *IEEE Journal on Selected Topics in Quantum Electronics*, vol. 6, p. 150-162, 2000.
- [4] Napartovich A.P., Elkin N.N., Sukharev A.G., Troshchieva V.N., Vysotsky D.V., Nesnidal M., Stiers E., Mawst L.J., Botez D., "Comprehensive Above-Threshold Analysis of Antiresonant Reflecting Optical Waveguide Edge-Emitting Diode Laser," *IEEE J. Quantum Electron.*, vol. 42, pp. 589-599, 2006.
- [5] G. R. Hadley, "Wide-angle beam propagation using Padé approximant operators," *Opt. Lett.*, vol. 17, p. 1426-1428, 1992.
- [6] W. P. Huang, C. G. Xu, W. Lui, and K. Yokoyama, "The Perfectly Matched Layer Boundary Condition for Modal Analysis of Optical Waveguides: Leaky Mode Calculations," *IEEE Photonics Technol. Lett.*, vol. 8, pp. 652 – 654, 1996.
- [7] N. N. Elkin, A. P. Napartovich, A. G. Sukharev, D. V. Vysotsky, "3D modeling of diode laser active cavity," *Lect. Notes in Comput. Science*, vol. 3401, pp.272–279, 2005
- [8] Demmel J., *Applied Numerical Linear Algebra*, Philadelphia, PA: SIAM, 1997.
- [9] A. Al-Muhanna, L. J. Mawst, D. Botez, D. Z. Garbuzov, R. U. Martinelli, J. C. Connolly, *Appl. Phys. Lett.*, vol. 73, pp. 1182-1184, 1998.